

See discussions, stats, and author profiles for this publication at: <https://www.researchgate.net/publication/231642062>

Ti(IV) Catalytic Centers Grafted on Different Siliceous Materials: Spectroscopic and Catalytic Study

ARTICLE *in* THE JOURNAL OF PHYSICAL CHEMISTRY C · MARCH 2007

Impact Factor: 4.77 · DOI: 10.1021/jp067506+

CITATIONS

60

READS

11

7 AUTHORS, INCLUDING:



Matteo Guidotti

Italian National Research Council

85 PUBLICATIONS 979 CITATIONS

SEE PROFILE



Nicoletta Ravasio

Italian National Research Council

132 PUBLICATIONS 1,942 CITATIONS

SEE PROFILE



Rinaldo Psaro

Italian National Research Council

231 PUBLICATIONS 4,234 CITATIONS

SEE PROFILE



Salvatore Coluccia

Università degli Studi di Torino

303 PUBLICATIONS 7,915 CITATIONS

SEE PROFILE

Ti(IV) Catalytic Centers Grafted on Different Siliceous Materials: Spectroscopic and Catalytic Study

Enrica Gianotti,^{*,†} Chiara Bisio,[‡] Leonardo Marchese,[‡] Matteo Guidotti,[§] Nicoletta Ravasio,[§] Rinaldo Psaro,[§] and Salvatore Coluccia[†]

Dipartimento di Chimica IFM and Centro di Eccellenza NIS, v. P. Giuria 7, 10125 Torino, Italy, A. Avogadro and Nano-SISTEMI Interdisciplinary Centre, Dipartimento di Scienza e Tecnologie Avanzate, and Nano-SISTEMI Interdisciplinary Centre, Università del Piemonte Orientale, A. Avogadro v. Bellini 25/G, 15100, Alessandria, Italy, and Istituto di Scienze e Tecnologie Molecolari and Centro di Eccellenza CIMAINA, CNR, via G. Venezian 21, Milano, Italy

Received: November 13, 2006; In Final Form: December 18, 2006

A detailed spectroscopic study was carried out on Ti(IV)-containing catalysts obtained by grafting titanocene dichloride on silica supports with different morphological features. The surface acidity and the local coordination and accessibility of Ti(IV) active centers in Ti(IV)-grafted materials were studied by FTIR and diffuse reflectance (DR) UV–vis–NIR spectroscopies supplemented by the use of probe molecules. DR UV–vis–NIR spectroscopy was also used to follow the formation of Ti(IV) catalytic sites and the removal of cyclopentadienyl moiety during thermal treatment. The use of CD₃CN and CO as molecular probes has provided complementary information on the accessibility and coordination of the Ti(IV) centers. In particular, CO adsorption performed at 100 K has evidenced the presence of Ti–OH groups and was helpful in detecting different coordination environments and connectivities of Ti(IV) active centers. Ti(IV)-grafted materials were tested in the epoxidation reaction of limonene using both *tert*-butyl hydroperoxide (TBHP) and H₂O₂ as oxidants. The interaction of TBHP or H₂O₂ with Ti(IV) active sites was investigated by DR UV–vis spectroscopy. This study has clarified that the use of H₂O₂ leads to a rapid and irreversible deactivation of the grafted Ti(IV) active sites; in fact, when H₂O₂ was used as oxidant no production of limonene oxide was detected.

1. Introduction

Titanium(IV)-containing silicas are of the utmost importance for their activity and their potential application in selective catalytic oxidations in the liquid phase. In particular, these catalysts are highly active in several reactions such as olefin epoxidation,¹ phenol oxidation,² and alcohol oxidation.³

Catalytic oxidation processes play an important role in the industrial production of fine chemicals, and the development of active and selective catalysts is an urgent need for some substrates, especially those using environmentally friendly oxidants such as H₂O₂ and alkyl hydroperoxides. A further improvement in the sustainability of such processes could be achieved by replacing the feedstocks derived from fossil raw materials with starting building blocks from renewables, such as carbohydrates, terpenes, and fatty acid derivatives. In this context, Ti(IV)-containing catalysts obtained by grafting titanocene dichloride (TiCp₂Cl₂) precursor onto the surface of silicas with different morphological features have shown attractive performances in the epoxidation not only of simple alkenes,^{4,5} but also of unsaturated terpenes⁶ and fatty acid methyl esters (FAMES) obtained from vegetable sources.^{7,8} In particular, Ti(IV) sites grafted onto the walls of a well-ordered mesoporous MCM-41 showed remarkably higher performances in the

selective epoxidation of fatty acid methyl esters than Ti(IV) centers grafted on nonordered mesoporous or nonporous silicas.^{7,8} This different catalytic behavior was attributed to the presence of a specific local environment of Ti(IV) sites, to their surroundings, and to the accessibility of the catalytic centers in MCM-41-based catalysts, as evidenced by the early work of Maschmeyer et al. using the extended X-ray absorption fine structure (EXAFS) technique.⁴ To achieve this information, it is also important to follow the formation of the catalytic Ti(IV) sites during thermal activation using *in situ* Fourier infrared (FTIR) and diffuse reflectance (DR) UV–vis–NIR spectroscopies. In addition, these techniques are also powerful tools to elucidate the local coordination, the dispersion, and the accessibility of the Ti(IV) active centers present in different silica materials.

To study the acidic properties of the Ti(IV)-containing silicas, FTIR spectroscopy of adsorbed molecules was used. Weak (CO, N₂),^{9–11} intermediate (CD₃CN),^{12,13} or strong (NH₃, pyridine)^{14,15} bases can be used as probe molecules.¹⁶ However, the interaction of weak and intermediate bases with catalytic surface sites are preferred because they are much more specific than strong bases.

In this paper, Brønsted and Lewis acidity of Ti(IV)-containing silicas was studied by FTIR and DR UV–vis spectroscopies using CO and CD₃CN as molecular probes. Since oxidation reactions occur thanks to the formation of oxygen-donating Ti(IV)–peroxo complexes, arising from the interaction of the oxidant on the tetrahedral Ti(IV) sites, this study is also devoted to investigating, by spectroscopic techniques, the interaction of the oxidants, i.e., *tert*-butyl hydroperoxide and hydrogen

* Corresponding author. Telephone: ++39-011-6705344. Fax: ++39-011-6707953. E-mail: enrica.gianotti@unito.it.

[†] Dipartimento di Chimica IFM.

[‡] Università del Piemonte Orientale.

[§] CNR.

TABLE 1: Textural Features and Titanium Loading of Ti(IV)-Containing Catalysts

catalyst	S_{BET}^a ($\text{m}^2 \text{g}^{-1}$)	D_p^b (nm)	Ti(IV) loading (wt %)
Ti-MCM-41	955	2.5	1.88
Ti-SiO ₂ Davison	303	12.7	1.75
Ti-SiO ₂ Aerosil	268	nd ^c	1.78

^a Specific surface area (from BET analysis). ^b Mean pore diameter.
^c Not determined.

peroxide normally used in liquid-phase oxidation reactions, with Ti(IV)-grafted silica catalysts.

2. Experimental Section

Titanocene dichloride (TiCp_2Cl_2) complex was used to functionalize silica material according to the procedure reported by Maschmeyer et al.⁴ and applied by some of us to other nonordered materials.¹⁷ TiCp_2Cl_2 was dissolved in chloroform and allowed to diffuse into MCM-41; the solid was then exposed in situ to triethylamine to activate the surface silanols. A well-ordered mesoporous MCM-41, a nonordered porous silica (Davison Grace), and a pyrogenic nonporous silica (Aerosil 380 Degussa) were studied. The Ti(IV) complexes were grafted onto the Si-OH surface groups after addition of triethylamine, and the Ti(IV) active centers were obtained after calcination in O₂ at 550 °C. These catalysts had similar Ti(IV) loading, as obtained from AES-ICP analysis. Specific surface area, pore dimensions, and Ti loading of the Ti(IV)-grafted silicas are reported in Table 1.

A purely siliceous mesoporous MCM-41 was synthesized according to a literature method using cetyltrimethylammonium bromide (CTMAB) as a structure directing agent.¹⁸ Before grafting titanium centers, the CTMAB surfactant was removed from the material at 550 °C, first under N₂ flow and subsequently under O₂.

FTIR spectra of self-supporting wafers of the samples (ca. 5 mg cm^{-2}) were recorded with a Bruker IFS88 spectrometer at a resolution of 4 cm^{-1} . Diffuse reflectance UV-vis-NIR spectra were collected by a Perkin-Elmer (Lambda 900) spectrometer equipped with an integrating sphere attachment. CD₃CN instead of CH₃CN was used as the probe molecule in order to avoid the Fermi resonance effect. To prevent any exchange of the deuterium atoms of CD₃CN with OH groups present at the surface of the materials, all samples were submitted to several D₂O vapor adsorption-desorption cycles at room temperature and finally treated under D₂ at 400 °C to deuterate all the surface OH groups. CD₃CN, anhydrous *tert*-butyl hydroperoxide (TBHP; 5–6 M in decane), and H₂O₂ (30 wt % aqueous solution) were adsorbed at room temperature, while CO was adsorbed at 100 K, using specially designed cells that were permanently connected to a vacuum line (ultimate pressure <10⁻⁵ Torr) to perform adsorption-desorption in situ experiments.

3. Results and Discussion

3.1. Formation of Ti(IV) Catalytic Sites. The evolution of surface species on Ti-MCM-41 from grafted Ti(IV)-cyclopentadienyl groups to grafted tetrahedral Ti(IV) active sites was followed by DR UV-vis-NIR spectroscopy. Figure 1 shows the UV-vis (A) and NIR (B) spectra of TiCp_2Cl_2 precursor grafted on the MCM-41. The sample was outgassed at increasing temperatures up to 350 °C (curves a–d) and, after the temperature was increased to 550 °C, calcined under O₂ at 550 °C

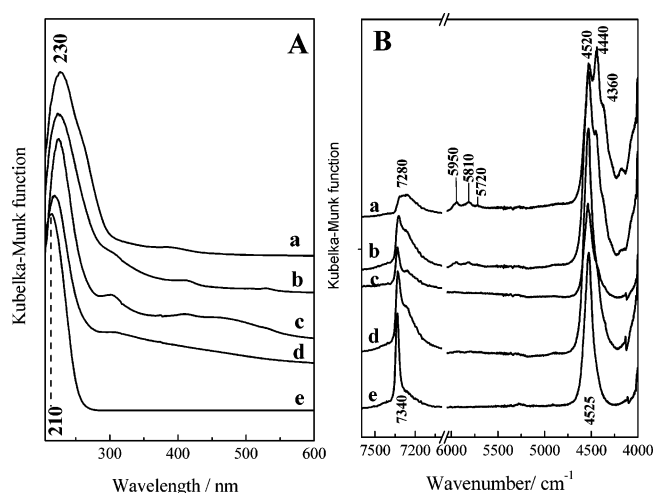


Figure 1. DR UV-vis (A) and NIR (B) spectra of cyclopentadienyl Ti(IV) species grafted onto MCM-41 outgassed at room temperature (a) and subsequently heated in vacuum at 150 (b), 250 (c), and 350 °C (d). Curve e refers to the sample calcined under O₂ at 550 °C.

(curve e). In the UV region, the spectrum of the sample outgassed at room temperature (curve a) shows a broad and intense absorption band at 230 nm with a broad shoulder at ca. 280 nm. A very weak signal at 400 nm is also found. By increasing the outgassing temperature (curves b and c), the broadness of the 230 nm band increases and features at higher wavelength become evident. In particular, signals at 300 nm and between 400 and 500 nm are visible in the spectrum of the sample outgassed at 250 °C (curve c) and can be due to species originated by the thermal decomposition of the cyclopentadienyl (CP) ligands.¹⁹ By increasing further the outgassing temperature up to 350 °C (curve d), the intense band at 230 nm shifts to 220 nm and becomes sharper, whereas the signals at higher wavelength almost completely disappear. This fact suggests that signals observed at ca. 280 nm and in the 400–500 nm range are due to organic species formed by the decomposition of CP ligands. Finally, the calcination of the sample at 550 °C (curve e) is capable of removing entirely the CP ligands and/or their decomposition products and leads to a material displaying a sharper and more intense absorption at 210 nm. The band at 210 nm is assigned to oxygen to tetrahedral Ti(IV) charge transfer (ligand to metal charge transfer, LMCT) transitions, and indicates that, in Ti-MCM-41, Ti(IV) sites exist mainly in tetrahedral coordination and are highly dispersed.^{20,21}

The vibrational features of the CP ligands along with those of the surface hydroxyls can be described considering the NIR region (Figure 1B). The sample outgassed at room temperature (curve a) shows a broad band at 7280 cm^{-1} , weak signals at 5950, 5810, and 5720 cm^{-1} , and a more complex absorption at lower frequencies with two peaks at 4520 and 4440 cm^{-1} , with the latter one having a shoulder at 4360 cm^{-1} . By increasing outgassing temperatures (curves b, c), the absorptions in the ranges 6000–5700 cm^{-1} and 4500–4300 cm^{-1} decrease in intensity and almost completely disappear at 250 °C (curve c) and more defined signals at ca. 7340 and 4525 cm^{-1} , with shoulders at 7260 and 4415 cm^{-1} , are formed. After calcination (curve e), only two narrow bands at 7340 and 4525 cm^{-1} are present. The band at the higher wavenumber is assigned to the first overtone of the stretching mode of free silanol groups ($2\nu_{\text{OH}}$), the fundamental being at 3745 cm^{-1} , and the latter is due to the combination of the deformation (δ_{OH} falling at around 785 cm^{-1})²² and the stretching OH modes ($\nu_{\text{OH}} + \delta_{\text{OH}}$).^{21,23–25} The Si-OH groups of the silica surface are the locus on which

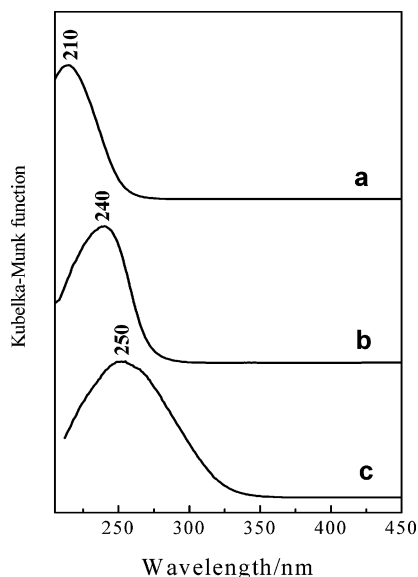


Figure 2. DR UV-vis spectra of calcined Ti-MCM-41 (a), Ti-SiO₂ Aerosil (b), and Ti-SiO₂ Davison (c).

the grafting of TiCp₂Cl₂ occurs, but, in order to react with the Ti(IV) complex, they have to be activated with Et₃N. In this step, triethylammonium chloride is produced along with cyclopentadiene and the monocyclopentadienyltitanium species are formed on the silica surface. In fact, after the grafting, the presence of a broad band at 7280 cm⁻¹ in the spectrum of outgassed sample at room temperature (curve a) indicates that almost all the Si-OH groups are involved in a proton transfer forming ⁺HNEt₃ species. However, a small fraction of silanols are involved in H-bonded surface species (broad band at 7280 cm⁻¹).

The evolution of the NIR spectra by increasing the temperature reveals that the signals at 5950 and 4440 cm⁻¹ are due to the first overtone of the C-H stretching mode (fundamental being at 2990 cm⁻¹) and to the combination of the deformation and the stretching C-H modes of the CP ligands, while the bands at 5810, 5720, and 4360 cm⁻¹ can be related to the first overtone of the asymmetric and symmetric stretching C-H modes (fundamentals at 2925 and 2855 cm⁻¹) and to the combination of the deformation with the asymmetric and symmetric stretching C-H modes of the triethylamine used to activate the Si-OH groups. These results indicate that calcination at high temperatures under oxygen is needed to remove not only the CP moieties grafted onto the silica surface, but also the residuals of triethylammonium chloride left after the grafting procedure and adsorbed on the porous materials.

The thermal activation was followed also on Ti-SiO₂ Davison and Ti-SiO₂ Aerosil catalysts (spectra not reported for the sake of brevity), and similar results were obtained; e.g., the CP ligands were decomposed after outgassing of the samples at 350 °C and the decomposition products were completely calcined under O₂ at 550 °C.

The DR UV-vis spectra of the calcined Ti-MCM-41 (curve a), Ti-SiO₂ Aerosil (curve b), and Ti-SiO₂ Davison (curve c) are reported in Figure 2. As described above, Ti-MCM-41 (curve a) shows a narrow UV band at 210 nm due to oxygen to tetrahedral Ti(IV) ligand to metal charge transfer (LMCT).^{20,21} There is an increasing broadness and a shift to higher wavelength of the UV absorption passing from Ti-SiO₂ Aerosil (curve b) to Ti-SiO₂ Davison (curve c). Bands at $\lambda \geq 230$ nm are consistent with an incipient oligomerization of Ti(IV) species.

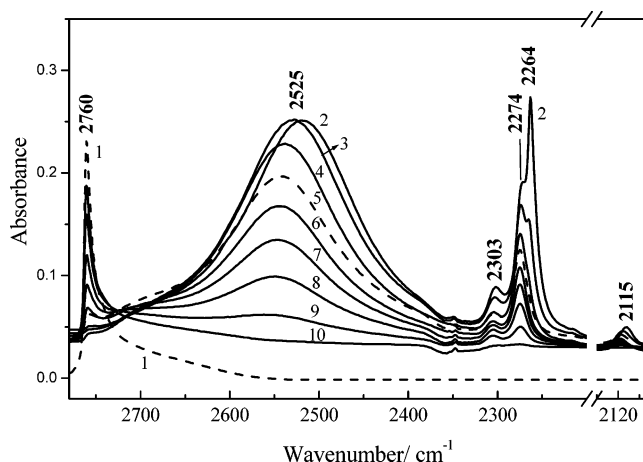


Figure 3. FTIR spectra of CD₃CN interaction on calcined Ti-MCM-41. (1) Deuterated sample outgassed at 500 °C in vacuum; (2) in contact with 100 Torr of CD₃CN; (3–9) decreasing doses of CD₃CN; (10) after evacuation at room temperature.

Ti-SiO₂ Aerosil (curve b) shows a broad band with a maximum at 240 nm that can be assigned to the presence of Ti-O-Ti dimeric species.²⁶

The broader absorption centered at 250 nm shown by Ti-SiO₂ Davison (curve c) evidences the presence, beside dimeric Ti(IV) species, of TiO₂-like clusters.^{20,21,26}

These data show that the grafting procedure is particularly efficient to generate well-spaced and structurally well-defined Ti(IV) isolated tetrahedral centers only when Ti(IV) complexes are grafted onto the walls of ordered silica MCM-41. In the case of siliceous supports with lower specific surface areas, i.e., SiO₂ Davison and SiO₂ Aerosil (Table 1), the Ti(IV)-grafting technique is less successful and noteworthy amounts of oligomeric and nontetrahedral Ti(IV) centers are present, even for relatively low titanium loadings (around 1.8 wt %).

3.2. Adsorption of CD₃CN and CO. The nature of the acid sites and the accessibility of Ti(IV) centers in Ti(IV)-grafted silicas was evaluated by acetonitrile adsorption at room temperature followed by FTIR and DR UV-vis-NIR spectroscopies. Acetonitrile is a widely used molecular probe because the stretching mode of the CN group is very sensitive to the acidity of the adsorption sites.^{13,27} In particular, when acetonitrile interacts with acid sites, the CN stretching mode shifts toward a higher wavenumber with respect to the molecule in the liquid phase; the stronger the interaction is between the CN group and acid sites, the larger is the shift. Deuterated acetonitrile (CD₃-CN) was used instead of CH₃CN to avoid Fermi resonance effects in FTIR spectra.

FTIR spectra of CD₃CN adsorbed on Ti-MCM-41 are reported in Figure 3. The narrow band at 2760 cm⁻¹ in the spectrum of the sample in a vacuum (curve 1) is due to the O-D stretching vibration of isolated deuteroyl groups formed after isotopic exchange with D₂O and D₂. Upon CD₃CN adsorption (vapor pressure ~100 Torr, curve 2), the band at 2760 cm⁻¹ almost completely disappears and new bands at 2525, 2303, 2274, 2264, and 2115 cm⁻¹ are formed.

The band centered at 2525 cm⁻¹ (very broad and strong) is assigned to the O-D stretching mode of deuteroyls D-bonded to CD₃CN molecules. The band at 2264 cm⁻¹, particularly intense at high CD₃CN pressure, is associated with physically adsorbed CD₃CN, and the band at 2274 cm⁻¹ is due to the C-N stretching mode of CD₃CN interacting with OD groups. The small blue shift ($\Delta\nu_{\text{CN}} = 12$ cm⁻¹) of the CN stretching mode produced by the interaction of CD₃CN with OD groups indicates

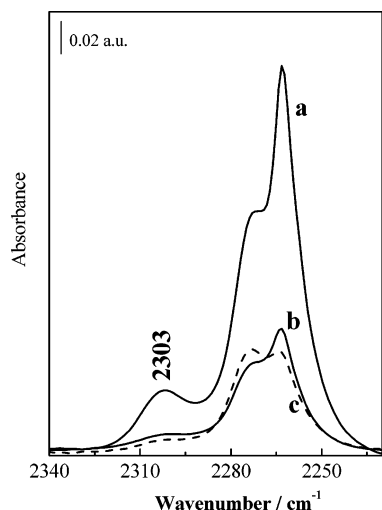


Figure 4. FTIR spectra of CD₃CN (vapor pressure \sim 100 Torr) adsorbed on Ti-MCM-41 (a), Ti-SiO₂ Aerosil (b) and Ti-SiO₂ Davison (c).

TABLE 2: Amount of CD₃CN Adsorbed on Ti(IV) Sites Measured by FTIR Spectroscopy

catalyst	adsorbed CD ₃ CN (cm ⁻¹ /mg cm ⁻²)	exposed Ti(IV) active sites (%)
Ti-MCM-41	0.6	100
Ti-SiO ₂ Aerosil	0.17	28
Ti-SiO ₂ Davison	0.15	25

that these OD groups have very low acidity, as expected for Si-OD groups. In fact, materials with strong Brønsted acid sites, such as zeolite H-ZSM-5, showed a shift of the ν_{CN} of 30–35 cm⁻¹.^{12,13,28} Nevertheless, such an acidic character, even if moderate with respect to that of zeolites, is enough to cause the acid-catalyzed cyclization of citronellal into isopulegol^{6,29} or the intramolecular ring closure of α -terpineol epoxide into 2-hydroxy-1,8-cineol.³⁰ The weak band at 2115 cm⁻¹ corresponds to the symmetric CD₃ stretching mode, which is less sensitive to the coordination of CD₃CN to surface centers.

The band at ca. 2303 cm⁻¹, particularly evident at high CD₃CN pressure, is associated with the CN stretching mode of acetonitrile directly bound to Ti(IV) Lewis acid sites. A band in a similar position was, in fact, observed upon CD₃CN adsorption both on TiO₂ anatase and on microporous TS-1, and it was assigned to the interaction of acetonitrile with uncoordinated Ti(IV) surface sites.^{12,31} According to the literature, acetonitrile is poorly sensitive to distinguish Ti(IV) sites in a different coordination environment.

All the bands due to adsorbed CD₃CN completely disappeared after outgassing of the sample at room temperature (curve 10).

The band at ca. 2303 cm⁻¹, associated with CD₃CN directly bound to Ti(IV) sites, is present, with differing intensity, on all Ti(IV)-grafted silica samples. Figure 4 shows the FTIR spectra of CD₃CN adsorbed (vapor pressure \sim 100 Torr) on Ti-MCM-41 (curve a), Ti-SiO₂ Aerosil (curve b), and Ti-SiO₂ Davison (curve c), in the CN stretching region. The band at 2264 cm⁻¹, associated with the physically adsorbed CD₃CN, is 3 times more intense on the Ti-MCM-41 sample with respect to the other Ti(IV)-silicas, due to the higher specific surface area (955 m² g⁻¹) of the MCM-41 support (Table 1). The values of the integrated area (cm⁻¹) of the 2303 cm⁻¹ band (Table 2), normalized to the thickness of the pellets (mg cm⁻²), for all samples were used to evaluate the amount of CD₃CN adsorbed

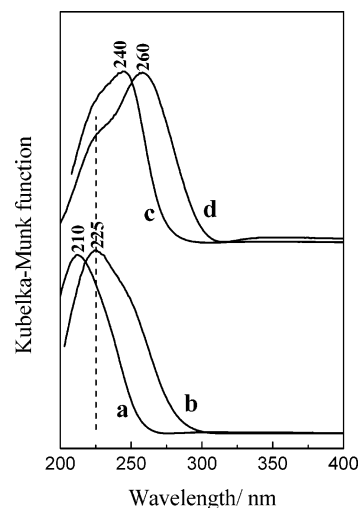


Figure 5. DR UV-vis spectra of calcined Ti-MCM-41 (a) and Ti-SiO₂ Aerosil (c). (b, d) Upon CD₃CN interaction at room temperature.

on Ti(IV) centers. This can be considered a way to measure and to quantify the fraction of Ti(IV) sites available for catalytic reactions.

Thanks to this method, the fraction of exposed and accessible Ti(IV) active sites can be evaluated. Assuming that all Ti(IV) sites are exposed and accessible (100% exposure) in Ti-MCM-41, in which almost all sites are in tetrahedral coordination, the FTIR data of adsorbed CD₃CN show that Ti-SiO₂ Aerosil has 28% and Ti-SiO₂ Davison has only 25% exposed Ti(IV) sites with respect to Ti-MCM-41. Therefore, the results of the catalytic tests carried out over materials with different morphologies can be normalized with respect to the fraction of active centers that effectively take part in the reaction and a real specific catalytic activity can be computed.

The accessibility of Ti(IV) sites is one of the main factors affecting the specific epoxidation activity of solid catalysts. Indeed, this effect is particularly evident on some substrates, such as unsaturated fatty acid methyl esters, where this order of the fraction of effectively exposed Ti(IV) sites reflects the activity of the heterogeneous catalysts.⁸ However, site accessibility is not the only factor determining the performances of Ti(IV)-based grafted catalysts. Actually, the site isolation, the morphology of the solid support, the hydrophilic-hydrophobic character of the local surroundings, and the stability of the surface Ti(IV) moieties toward degradation and/or leaching are all key points whose balance ought to be taken into account in order to obtain a system with significant catalytic performances.

CD₃CN interaction with Ti(IV) active sites was also investigated by DR UV-vis spectroscopy (Figure 5). The band at 210 nm (curve a), due to the LMCT transition of tetrahedral Ti(IV) sites, broadened and shifted to 225 nm upon acetonitrile adsorption (curve b), suggesting that Ti(IV) sites have expanded their coordination sphere.³² The CD₃CN adsorption was also followed on Ti-SiO₂ Aerosil catalyst. In this case, the band at 240 nm in the calcined sample (curve c) and due to the presence of Ti-O-Ti dimeric species, broadened and shifted to 260 nm and a shoulder at lower wavelength (ca. 225 nm) is visible after CD₃CN interaction (curve d). The red shift of the band at 240 nm is a signal that also Ti(IV) sites in Ti-O-Ti dimeric species have some coordination vacancies able to bind CD₃CN molecules. This is a clue that these Ti(IV) dimeric species are potentially able to coordinate organic peroxide species and hence are able to take part in the epoxidation process. Moreover, the presence of the shoulder at lower wavelength in the same

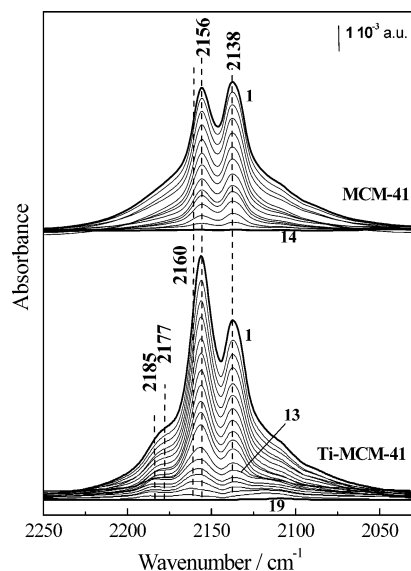


Figure 6. FTIR spectra of CO adsorbed at 100 K on calcined MCM-41 (top) and Ti-MCM-41 (bottom). Curves 1–14 for MCM-41 and curves 1–19 for Ti-MCM-41 correspond to decreasing CO pressure from 40 to 10^{-3} mbar (residual pressure after evacuation at room temperature).

position of the one observed after CD_3CN interaction on Ti(IV) sites in Ti-MCM-41 (curve b) suggests that, also in Ti-SiO₂ Aerosil, tetrahedral Ti(IV) centers are present. These tetrahedral sites are masked by the broad absorption centered at 240 nm due to more coordinated Ti(IV) sites and become visible when tetrahedral Ti(IV) sites expand their coordination sphere after the adsorption of CD_3CN molecules.

Beside CD_3CN adsorption, the acid properties of pure MCM-41 and of the Ti(IV) sites in both Ti-MCM-41 and Ti-SiO₂ Aerosil were studied using carbon monoxide as a probe molecule.

Figure 6 shows FTIR spectra of CO adsorbed at 100 K on pure MCM-41 (top) and on calcined Ti-MCM-41 (bottom). Two bands at 2156 and 2138 cm^{-1} are present in the spectra of CO adsorbed at 100 K on MCM-41 (curve 1, top). The band at 2138 cm^{-1} is due to physically adsorbed CO. The band at 2156 cm^{-1} decreases in intensity upon CO evacuation (curves 1–14) contemporaneously with the reappearance of the band at 3745 cm^{-1} (range not shown), typical of the O–H stretching mode of free hydroxyl groups. This band is therefore associated with the C–O stretching mode of CO interacting by H-bonding with Si–OH groups. The bands at 2156 and 2138 cm^{-1} are present in the FTIR spectra of CO adsorbed at 100 K on Ti-MCM-41 (Figure 6, bottom) together with a new band at 2177 cm^{-1} , which shifts to 2185 cm^{-1} with decreasing CO pressure. Bands in the 2200–2170 cm^{-1} range are assigned to the C–O stretching mode of CO adsorbed on Ti(IV) Lewis acid sites.^{33,34}

The band at 2156 cm^{-1} , associated with C–O stretching of carbon monoxide H-bonded with OH groups, has a strong shoulder on the high-frequency side (ca. 2160 cm^{-1}), particularly evident at lower CO dosages (curve 13), that is not present in the FTIR spectra of CO adsorbed on MCM-41 (Figure 6, top). It is proposed that the feature is related to a direct interaction of CO molecules with OH groups of titanols (Ti–OH) that are formed after calcination of the sample at 550 °C.^{4,20,21} This is a very interesting observation as it is not easy to distinguish the vibrations of titanols in the OH stretching region because it is strongly overlapped to the vibrations of Si–OH, which are very abundant in Ti-MCM-41.

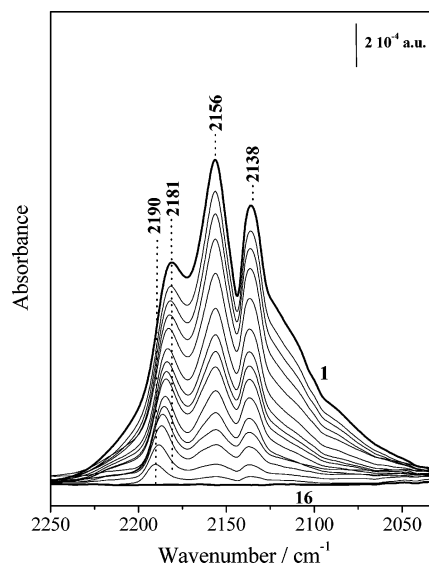


Figure 7. FTIR spectra of CO adsorbed at 100 K on calcined Ti-SiO₂ Aerosil. Curves 1–16 correspond to decreasing CO pressure from 40 to 10^{-3} mbar (residual pressure after evacuation at room temperature).

The bands at 2156 and 2138, although with lower intensity, are also present after CO adsorption at 100 K on Ti-SiO₂ Aerosil catalyst (Figure 7). The band associated with CO interaction with Ti(IV) Lewis centers is present at 2181 cm^{-1} and shifts to 2190 cm^{-1} at low CO dosages. The higher frequencies of the bands, associated with the CO interaction on Ti(IV) sites, suggested a different nature of Ti(IV) centers in Ti-SiO₂ Aerosil.

CO is completely removed after outgassing of the samples at 100 K for 15 min on both Ti-MCM-41 and Ti-SiO₂ Aerosil.

Bands in the range 2200–2170 cm^{-1} were also found in the FTIR spectra of CO adsorbed on TiO₂–SiO₂ mixed oxides³³ and on Ti-HMS materials.³⁴ The presence of two set of bands, at 2199–2185 cm^{-1} and at 2177–2173 cm^{-1} , was attributed to the existence of two types of Ti(IV) sites. The first type (2199–2185 cm^{-1}) was attributed to Ti(IV) sites having at least one additional Ti(IV) cation in their second coordination sphere, whereas the second one (2177–2173 cm^{-1}) was assigned to isolated Ti(IV) centers. For both types of Ti(IV) sites, the bands shifted to higher frequency by decreasing of the CO pressure. On the basis of the literature data, we assigned the band at 2190–2181 cm^{-1} , in the FTIR spectra of Ti-SiO₂ Aerosil, to CO adsorbed on Ti(IV) sites with one additional Ti(IV) cation in the second coordination sphere and the band at 2185–2177 cm^{-1} , in the FTIR spectra of Ti-MCM-41, to CO adsorbed on Ti(IV) tetrahedral isolated centers. These results are in good agreement with the data obtained by the DR UV–vis studies that have evidenced the presence of well-isolated tetrahedral Ti(IV) sites in Ti-MCM-41 and a large amount of species with Ti–O–Ti connectivity in Ti-SiO₂ Aerosil (see Figure 2). Carbon monoxide is therefore a very sensitive probe molecule to monitor different coordination environments of Ti(IV) Lewis sites and to evaluate the differences in its second coordination sphere.

3.3. Adsorption of *tert*-Butyl Hydroperoxide and Hydrogen Peroxide. In the epoxidation reactions carried out over Ti(IV)-containing silicates, H₂O₂ and TBHP are normally used as oxidants. The interaction of the oxidant with the Ti(IV) centers and the nature of the peroxo complexes formed are crucial to understanding the epoxidation mechanism and to estimating the stability of the resulting catalyst/oxidant adduct.

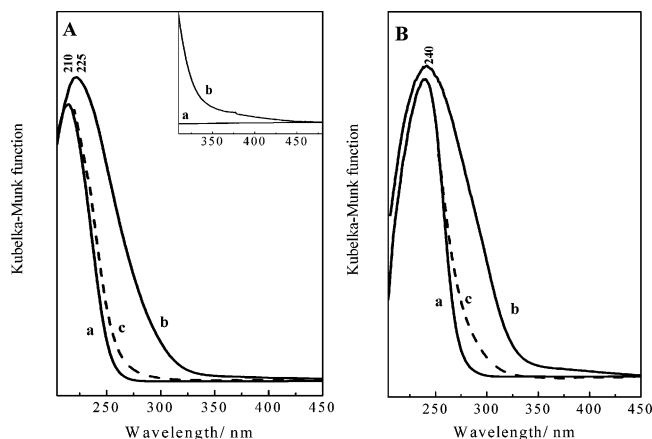
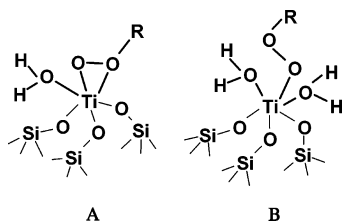


Figure 8. DR UV-vis spectra of calcined Ti-MCM-41 (A, curve a) and Ti-SiO₂ Aerosil (B, curve a), after TBHP adsorption at room temperature (b), and after reactivation in O₂ at 550 °C (c).

SCHEME 1



Anhydrous TBHP was left in contact with Ti-MCM-41 and Ti-SiO₂ Aerosil catalysts at room temperature for 1 h. Both samples turned pale yellow, and this is direct evidence that Ti(IV)-peroxo complexes were formed.³⁵ Figure 8A reports the DR UV-vis spectra of Ti-MCM-41 before and after TBHP interaction. The adsorption of TBHP on calcined Ti-MCM-41 produced a shift of the band at 210 nm (curve a), typical of Ti(IV) tetrahedral centers, to higher wavelength (curve b). The same effect was also observed upon CD₃CN interaction, and it is due to an expansion of the coordination sphere of Ti(IV) tetrahedral sites. Moreover, in this case, a very weak and broad signal appeared around 350–450 nm (see inset of Figure 8A, curve b). This signal is assigned to a ligand to metal charge transfer (LMCT) transition from the peroxidic moiety to Ti(IV) active centers.^{35–38} A signal in a similar position was also found in the DR UV-vis spectrum of Ti-SiO₂ Aerosil after TBHP contact (Figure 8B, curve b). After reactivation in O₂ at 550 °C (curves c in Figure 8A,B), the features related to the presence of Ti(IV)-peroxo species are completely removed and the original adsorption edge is almost entirely restored for Ti-MCM-41, whereas a broader tail is still present on the high-wavelength side of the 240 nm band of Ti-SiO₂ Aerosil. The nature of the Ti(IV)-peroxo complexes in grafted Ti-MCM-41 using TBHP was studied by Barker et al. by means of EXAFS and density functional theory calculation.³⁹ The comparison of theory with experiment suggests that an oxygen-donating species is 6-coordinated with both η^2 -OO'Bu (Scheme 1, structure A) and η^1 -OO'Bu species (Scheme 1, structure B).

On the other hand, when H₂O₂ is left in contact with Ti(IV)-grafted silicas, the UV-vis spectra of both samples change irreversibly. Figure 9A shows the DR UV-vis spectra of Ti-MCM-41 sample before and after H₂O₂ adsorption. The band at 210 nm due to tetrahedral Ti(IV) centers (curve a) broadened and shifted to 250 nm upon H₂O₂ contact (curve b). This shift is larger than the one observed upon TBHP interaction attributed to the formation of 6-coordinated Ti(IV) species. After

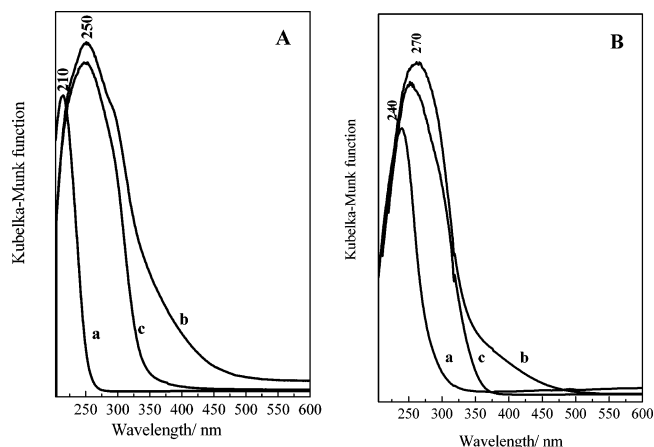


Figure 9. DR UV-vis spectra of calcined Ti-MCM-41 (A, curve a) and Ti-SiO₂ Aerosil (B, curve a), after H₂O₂ adsorption at room temperature (b), and after reactivation in O₂ at 550 °C (c).

TABLE 3: Performances of Ti-MCM-41 in the Liquid-Phase Epoxidation of Limonene

catalytic test	treatment	oxidant ^a	conv ^b (%)	sel ^c (%)
1	air; 1 h; 500 °C	TBHP	77	81
2	air; 1 h; 500 °C	H ₂ O ₂	18	ca. 0
3	air; 1 h; 500 °C	TBHP	20	80
	H ₂ O ₂ in CH ₃ CN; 30 min ^d drying at 90 °C			
4	air; 1 h; 500 °C	TBHP	30	77
	H ₂ O ₂ in CH ₃ CN; 30 min ^d air; 1 h; 500 °C			

^a In all cases: 1.0 mmol of limonene; 1.1 mmol of oxidant; 21 μ mol of Ti; 5 mL of CH₃CN. ^b Conversion of limonene (mol %) after 24 h. ^c Selectivity to endocyclic limonene oxide. ^d Concentrations and conditions similar to those of catalytic tests.

the reactivation of the catalysts in O₂ at 550 °C (curve c), the original absorption maximum at 210 nm is not restored and a relevant fraction of species absorbing in the range 300–350 nm is still present. This spectroscopic behavior suggests that, upon H₂O₂ interaction, hydrolysis of Ti–O–Si bonds and aggregation of Ti(IV) centers, forming TiO_x-like species, occur. The same effect was observed after H₂O₂ adsorption on Ti-SiO₂ Aerosil (Figure 9B). Also in this case, H₂O₂ modified irreversibly the Ti(IV) centers producing TiO₂-type aggregates. A similar behavior was also observed on a Ti-MCM-41 in which titanium sites were introduced by impregnation.⁴⁰ These results evidenced that H₂O₂ is not a suitable oxidant for the epoxidation of poorly reactive substrates using Ti(IV)-grafted silicas as catalysts because a rapid and irreversible transformation of isolated centers into oxide-like titanium species takes place.

This spectroscopic evidence prompted us to plan a tailored set of experiments in order to verify the irreversible modification of the Ti(IV) centers upon H₂O₂ interaction. The unsaturated terpene limonene was chosen as a test substrate because in preliminary studies it was shown to be readily epoxidized by TBHP,^{6,25} but almost completely inactive with H₂O₂ (Table 3). Indeed, Ti-MCM-41 is an efficient catalyst in the presence of TBHP as oxidant (entry 1), whereas it is almost completely inactive when H₂O₂ is used (entry 2). More exactly, small conversion values of the reactant were recorded with H₂O₂ as oxidant, but no production of limonene oxide (the compound directly obtained by epoxidation of limonene) was detected. Furthermore, if the catalyst is first treated with a mixture of

H₂O₂ in acetonitrile (with a concentration identical to the reaction conditions, but without limonene), dried, and used in a new catalytic run with TBHP (entry 3), only a very small production of limonene oxide is recorded. The initial activity of the catalyst is also not restored, using TBHP as oxidant, if the catalyst, treated with H₂O₂ in acetonitrile, is calcined at 500 °C for 1 h under air (entry 4). This behavior indicates that, after H₂O₂ contact, the catalyst is irreversibly modified and deactivated. The spectroscopic evidence and the catalytic tests therefore confirm that the inactivity of Ti(IV)-grafted materials with H₂O₂ as oxidant is not due to the irreversible adsorption of inhibiting species (which could be otherwise removed by calcination), but rather to an irreversible modification of the Ti(IV) catalytic sites.

4. Conclusions

The formation of Ti(IV) active centers grafted on silica supports with different morphological features and local coordination was investigated by DR UV–vis–NIR spectroscopy. The decomposition of the cyclopentadienyl ligands occurs at temperatures above ca. 350 °C for all samples, producing Ti(IV) centers that present a different degree of dispersion depending on the silica support used. A clean surface was obtained only after calcination under O₂ at 550 °C. In particular, well-dispersed and tetrahedral Ti(IV) sites were obtained by grafting titanocene dichloride onto the walls of mesoporous MCM-41. The adsorption of molecular probes, such as CO and acetonitrile, followed by FTIR and DR UV–vis–NIR, gave information on the acidity and the accessibility of Ti(IV) Lewis active sites in different Ti(IV)-grafted catalysts. In particular, acetonitrile was found to be a useful molecular probe to monitor the accessibility of Ti(IV) sites, and the adsorption of deuterated acetonitrile can be an effective method for the quantification of exposed Ti(IV) centers. The use of this molecule can provide the necessary information for the evaluation of the actual catalytic specific activity in Ti(IV)-containing catalysts. However, CD₃CN is limited in distinguishing Ti(IV) sites with a different coordination. Otherwise, carbon monoxide helps in detecting different coordination environments and connectivities of Ti(IV) active sites. In addition, the adsorption of CO at 100 K is also able to reveal the presence of Ti–OH groups in Ti(IV)-grafted MCM-41.

Last, the experiments on the interaction of TBHP and H₂O₂ with Ti(IV) centers have clarified that H₂O₂ leads to a rapid and irreversible transformation of Ti(IV) centers into oxide-like titanium species, which were found not catalytically active in the epoxidation of limonene.

Acknowledgment. The authors are grateful to the European Commission for the financial support by means of the Specific Targeted Research Or Innovation Project (STRP) project “Nanofire”—Proposal No. 505637-1 in the context of the 6th Framework Programme. The authors also thank Compagnia di San Paolo for sponsorship to NIS and Ms. Maila Sgobba for the catalytic tests.

References and Notes

- (1) De Vos, D. E.; Sels, B. F.; Jacobs, P. A. *Adv. Synth. Catal.* **2003**, *345*, 457.
- (2) Kholdeeva, O. A.; Melgunov, M. S.; Shmakov, A. N.; Trukhan, N. N.; Kriventsov, V. V.; Zaikovskii, V. I.; Romannikov, V. N. *Catal. Today* **2004**, *91–92*, 205.
- (3) Arends, W. C. E.; Sheldon, R. A.; Wallau, M.; Schuchardt, U. *Angew. Chem., Int. Ed.* **1997**, *36*, 1144.
- (4) Maschmeyer, T.; Rey, F.; Sankar, G.; Thomas, J. M. *Nature* **1995**, *378*, 159.
- (5) Oldroyd, R. D.; Thomas, J. M.; Maschmeyer, T.; MacFaul, P. A.; Snelgrove, D. W.; Ingold, K. U.; Wayner, D. D. M. *Angew. Chem., Int. Ed.* **1996**, *35*, 2787.
- (6) Guidotti, M.; Ravasio, N.; Psaro, R.; Ferraris, G.; Moretti, G. *J. Catal.* **2003**, *214*, 242.
- (7) Guidotti, M.; Ravasio, N.; Psaro, R.; Gianotti, E.; Marchese, L.; Coluccia, S. *Green Chem.* **2003**, *5*, 421.
- (8) Guidotti, M.; Ravasio, N.; Psaro, R.; Gianotti, E.; Marchese, L.; Coluccia, S. *J. Mol. Catal. A: Chem.* **2006**, *250*, 218.
- (9) Knözinger, H.; Huber, S. J. *Chem. Soc., Faraday Trans.* **1998**, *94*, 2047.
- (10) Smith, L.; Cheetham, A. K.; Marchese, L.; Thomas, J. M.; Wright, P. A.; Chen, J.; Gianotti, E. *Catal. Lett.* **1996**, *41*, 13.
- (11) Wakabayashi, F.; Kondo, J. N.; Wada, A.; Domen, K.; Hirose, C. *J. Phys. Chem.* **1996**, *100*, 18882.
- (12) Bonino, F.; Damin, A.; Bordiga, S.; Lamberti, C.; Zecchina, A. *Langmuir* **2003**, *19*, 2155.
- (13) Pelmenchikov, A. G.; van Santen, R. A.; Janchen, J.; Meijer, E. *J. Phys. Chem.* **1993**, *97*, 1107.
- (14) Pazè, C.; Bordiga, S.; Lamberti, C.; Salvalaggio, M.; Zecchina, A.; Bellussi, G. *J. Phys. Chem. B* **1997**, *101*, 4740.
- (15) Zecchina, A.; Marchese, L.; Bordiga, S.; Pazè, C.; Gianotti, E. *J. Phys. Chem. B* **1997**, *101*, 10129.
- (16) Coluccia, S.; Marchese, L.; Martra, G. *Microporous Mesoporous Mater.* **1999**, *30*, 43.
- (17) Guidotti, M.; Conti, L.; Fusi, A.; Ravasio, N.; Psaro, R. *J. Mol. Catal. A: Chem.* **2002**, *182–183*, 215.
- (18) Kresge, C. T.; Leonowicz, M. E.; Roth, W. J.; Vartuli, J. C.; Beck, J. S. *Nature* **1992**, *359*, 710.
- (19) Calleja, G.; van Grieken, R.; Garcia, R.; Melero, J. A.; Iglesias, J. *J. Mol. Catal. A: Chem.* **2002**, *182–183*, 215.
- (20) Marchese, L.; Maschmeyer, T.; Gianotti, E.; Coluccia, S.; Thomas, J. M. *J. Phys. Chem. B* **1997**, *101*, 8836.
- (21) Marchese, L.; Gianotti, E.; Dellarocca, V.; Maschmeyer, T.; Rey, F.; Coluccia, S.; Thomas, J. M. *Phys. Chem. Chem. Phys.* **1999**, *1*, 585.
- (22) Burbeau, A.; Gallas, J.-P. *The Surface Properties of Silicas*; Legrand, A. P., Ed.; Wiley: Chichester, U.K., 1998; p 147.
- (23) Anderson, J. H., Jr.; Wickersheim, K. A. *Surf. Sci.* **1964**, *2*, 252.
- (24) Morrow, B. A.; McFarlan, A. J. *J. Phys. Chem.* **1992**, *96*, 1395.
- (25) Peña, M. L.; Dellarocca, V.; Rey, F.; Corma, A.; Coluccia, S.; Marchese, L. *Microporous Mesoporous Mater.* **2001**, *44–45*, 345.
- (26) Gianotti, E.; Frache, A.; Coluccia, S.; Thomas, J. M.; Maschmeyer, T.; Marchese, L. *J. Mol. Catal. A: Chem.* **2003**, *204–205*, 483.
- (27) Chen, J.; Thomas, J. M.; Sankar, G. *J. Chem. Soc., Faraday Trans.* **1994**, *90*, 3455.
- (28) Otero Areán, C.; Escalona Platero, E.; Peñarroya, M.; Mentruit, M.; Rodriguez Delgado, M.; Llabrés i Xamena, F.; Garcia-Raso, A.; Morterra, C. *Microporous Mesoporous Mater.* **2000**, *34*, 55.
- (29) Guidotti, M.; Moretti, G.; Psaro, R.; Ravasio, N. *Chem. Commun.* **2000**, 1789.
- (30) Berlino, C.; Guidotti, M.; Moretti, G.; Psaro, R.; Ravasio, N. *Catal. Today* **2000**, *60*, 219.
- (31) Davit, P.; Martra, G.; Coluccia, S.; Augugliaro, V.; Garcia-Lopez, E.; Lodo, V.; Marci, G.; Palmisano, L.; Schiavello, M. *J. Mol. Catal. A: Chem.* **2003**, *204–205*, 693.
- (32) Gianotti, E.; Marchese, L.; Guidotti, M.; Ravasio, N.; Psaro, R.; Coluccia, S. *Stud. Surf. Sci. Catal.* **2005**, *155*, 311.
- (33) Hadjiivanov, K.; Reddy, B. M. Knözinger, H. *Appl. Catal. A: Gen.* **1999**, *188*, 355.
- (34) Trukhan, N. N.; Panchenko, A. A.; Roduner, E.; Mel'gunov, M. S.; Kholdeeva, O. A.; Mrowiec-Bialon, J.; Jarzebski, A. B. *Langmuir* **2005**, *21*, 10545.
- (35) Bordiga, S.; Damin, A.; Bonino, F.; Ricchiardi, G.; Lamberti, C.; Zecchina, A. *Angew. Chem., Int. Ed.* **2002**, *41*, 4734.
- (36) Bonino, F.; Damin, A.; Ricchiardi, G.; Ricci, M.; Spanò, G.; D'Aloisio, R.; Zecchina, A.; Lamberti, C.; Prestipino, C.; Bordiga, S. *J. Phys. Chem. B* **2004**, *108*, 3573.
- (37) Shetti, V. N.; Manijandan, P.; Srinivas, D.; Ratnasamy, P. *J. Catal.* **2003**, *216*, 461.
- (38) Srinivas, D.; Manijandan, P.; Laha, S. C.; Kumar, R.; Ratnasamy, P. *J. Catal.* **2003**, *217*, 160.
- (39) Barker, C. M.; Gleeson, D.; Kaltsayannis, N.; Catlow, C. R. A.; Sankar, G.; Thomas, J. M. *Phys. Chem. Chem. Phys.* **2002**, *4*, 1228.
- (40) Hagen, A.; Schueler, K.; Roessner, F. *Microporous Mesoporous Mater.* **2002**, *51*, 23.